4

Molecular Beam Epitaxy Growth of Nanowires in the $Hg_{1-x}Cd_xTe$ Material System

Randi Haakenaasen and Espen Selvig
Norwegian Defence Research Establishment
Norway

1. Introduction

The size of electronic components keeps decreasing as more computing power is packed into the volume of a personal computer. There are also clear advantages to shrinking sensors and other electronic devices; they will be lighter, smaller and require less power. More functionality can then be added to portable instruments, whether they are cellular phones or uniforms for soldiers. In the quest for miniaturization, nanotechnology is an obvious field of study. Nanostructures can have properties that differ from those of the bulk material, for example size-tunable effective band gap or high sensitivity to surface preparation due to the large surface-to-volume ratio. This can lead to miniaturized components with completely new properties.

Nanowires are today grown in numerous material systems such as GaAs, Si, GaP, InP, ZnS, CdSe, ZnTe or GaAsSb (Olsson *et al.*, 2001; Duan & Lieber, 2000; Shan *et al.*, 2005; Janik *et al.*, 2006; Dheeraj *et al.*, 2008). Most of these are grown with vapor phase epitaxy techniques using the vapor-liquid-solid (VLS) or vapor-solid-solid (VSS) mechanism, in which the component fluxes go through or around a gold catalyst particle and the nanowire grows underneath this particle (Wagner & Ellis, 1964; Persson *et al.*, 2004). Many groups have also successfully grown segmented or heterostructured nanowires (Björk *et al.*, 2002; Wu *et al.*, 2002; Gudiksen *et al.*, 2002). Various nanowire devices have been demonstrated, for example a *pn* junction, field-effect transistor, photodetector, polarized light emitting diode (LED), laser, single electron transistor, optical switch, and detectors for biological and chemical molecules.

$Hg_{1-x}Cd_xTe$ is an alloy between the semimetal HgTe and the semiconductor CdTe, and it has a direct band gap that is tunable from -0.26 eV (HgTe) to 1.61 eV (CdTe) at 77 K, covering the entire infrared (IR) region. The small effective electron mass of $Hg_{1-x}Cd_xTe$ (minimum of about 0.02 m_0 for $Hg_{0.66}Cd_{0.34}Te$) leads to a quantum upshift for larger structures than in other materials and enables size-tunable electrical and optical properties. In HgTe particles there should, for example, be quantum effects for diameters smaller than 80 nm and a positive band gap below 18 nm (Green *et al.*, 2003). HgCdTe is mostly used for high performance IR detectors, but the small lattice mismatch in this material system (maximum 0.3% between CdTe and HgTe), facilitates growing heterostructures, including quantum wells, with good crystallinity (Tonheim *et al.*, 2008). Hg(Cd)Te also has a number of other

Source: Nanowires, Book edited by: Paola Prete,
ISBN 978-953-7619-79-4, pp. 414, March 2010, INTECH, Croatia, downloaded from SCIYO.COM

special properties which make it appealing to explore nanostructures in this material system: it is piezoelectric and it has high electron mobility, high dielectric constant, large *g*-factor, large spin-orbit coupling, and Rashba effect. Many of these properties are strongly correlated with the fraction of HgTe in the material. HgTe is, for example, a candidate for spintronics applications, and a quantum spin Hall effect has been discovered in HgTe quantum wells (König *et al*., 2007). HgTe is also a thermoelectric material, and recently nanomaterials have shown potential in improving thermoelectric materials. Enhanced thermoelectric performance in one-dimensional segmented nanowire systems has been demonstrated in $Bi/Bi_{1-x}Sb_x$ nanowires (Dresselhaus *et al*., 2003). Possible interesting HgTe and HgCdTe nanowire electro-optical applications include polarization-sensitive detectors, detectors with reduced cooling requirements, lasers and LEDs in the infrared region of the spectrum.

Recently, HgTe nanorods have been synthesized in solution (Song *et al*., 2004; Qin *et al*., 2007) or formed within single wall carbon nanotubes (Carter *et al*., 2006), and HgTe nanotubes have been prepared by spray deposition of solvothermally synthesized iodine-doped HgTe nanoparticles (Ranga Roa & Dutta, 2006). HgCdTe nanorods (up to 300 nm long) have been made by adding Hg^{2+} ions into a solution containing CdTe nanorods (Tang *et al*., 2007). Networks or nanowires of HgCdTe nanoparticles have also been produced by dissolving CdTe nanoparticles in a solution containing Hg^{2+} ions (Yang *et al*., 2009). As the Hg is added by in-diffusion in solution, a gradient in the composition within the nanowire is expected. Room temperature absorption and PL spectra showed peaks in the range 700 - 1200 nm. Photo detection was demonstrated as an incident light (λ = 785 nm) changed the conductivity of the network with a rise and fall time of 2 s.

The motivation for using molecular beam epitaxy (MBE) to grow HgTe and HgCdTe nanowires is that, although MBE growth of Hg(Cd)Te is both complicated and challenging, its high precision and flexibility can give good control over the growth of thin layers and abrupt junctions, which may be an advantage in future nanostructure devices. Furthermore, MBE growth of HgTe and HgCdTe thin films occurs near thermal equilibrium (~200 ^{o}C), and the Hg atoms re-evaporate easily while the Te atoms are very mobile on the surface (Selvig *et al*., 2008a). This offers the potential for self-organized growth of crystals for deposition rates lower than during thin film growth.

Three different techniques have been tested to make HgTe and HgCdTe nanowires, namely self-organization (without a catalyst), VLS and using SiO_2 as a mask material for selective growth. Three types of HgTe nanowires have been grown: **I**) thick, polycrystalline HgTe wires, **II**) thin, twisted, <111>-oriented single crystal HgTe nanowires, and **III**) thin, straight, segmented HgTe<111>/Te<001> nanowires (Hadzialic, 2004; Selvig *et al*., 2006; Haakenaasen *et al*., 2008a; Haakenaasen *et al*., 2008b). The HgTe wires do not grow by the VLS mechanism. Instead, small Au particles function as nucleation sites for the wires, which subsequently self-organize and grow laterally on the substrate, without epitaxial coupling to the latter. Te and Au nanowires were also fabricated. Attempts at growing HgCdTe nanowires by MBE have not been successful (Haakenaasen *et al*., 2008a). A comparison with the phase diagrams for the GaAs material system offers an explanation for why HgCdTe/HgTe nanowires were not obtained by the VLS technique. SiO_2 functions as a mask material for HgTe, but not for HgCdTe. Conductive atomic force microscopy has been used to measure the resistivity of the polycrystalline type I HgTe nanowires.

2. Experimental

Si(100), GaAs(100) or $Cd_{0.96}Zn_{0.04}Te$ (100), (111)B and (211)B substrates were used. The substrates were generally wet-etched to remove oxides from the surface. Si and GaAs substrates were etched in hydrofluoric acid (1:10, 48% HF:H_2O) for 3 s and CdZnTe substrates were etched in a (1:100, Br:methanol) solution for 2 min. In the attempts at self-organized growth without a catalyst, some of the substrates were scratched with either a clean q-tip or a q-tip dipped in an 1-μm-diamond-slurry before wet-etching, while some were just etched. Some samples were partly covered by a sputtered layer of SiO_2. For the attempts at VLS growth, the substrates were etched and loaded into a sputtering machine where a ~ 5-60 Å thick layer of Au was deposited. The substrates were then loaded into a Riber 32P MBE machine and heated to 340°C for 10 minutes, resulting in break-up of the gold film into particles of diameter 2-50 nm. Some Si substrates were covered with a photoresist mask (for example an array of 3.5-μm-diameter holes) and the HF etch repeated before Au sputtering, resulting in Au particles in defined areas only.

MBE growth of HgTe and HgCdTe thin films of high crystalline quality requires controlling the substrate temperature to within ± 1°C of the optimum growth temperature, which is just below the Te-phase limit (onset of Te precipitation) (Colin & Skauli, 1997; Selvig *et al.*, 2007; Selvig *et al.* 2008a; Selvig *et al.*, 2008b). In our MBE machine this is 193°C for HgTe and 198°C for $Hg_{0.75}$ $Cd_{0.25}Te$. The growth rate is determined by the Te flux while the Hg flux is kept constant. The growth conditions for the nanowire experiments were similar to those used for HgTe or HgCdTe films grown on CdZnTe(211)B substrates except for lower growth temperatures (178, 186, or 188 °C for HgTe, 192 - 193°C for $Hg_{0.75}$ $Cd_{0.25}Te$, 335°C for CdTe) and much lower deposition rates (would give equivalent thin film growth rates in the range 1-100 Å/min). The equivalent film thickness deposited was varied from 20 Å to 0.5 μm in order to investigate how the nanowires evolve during growth. Below we will take 'deposition rate' to mean 'equivalent thin film growth rate'.

The grown samples were investigated with scanning electron microscopy (SEM), energy dispersive x-ray spectroscopy (EDX), x-ray photoelectron spectroscopy (XPS), and transmission electron microscopy (TEM). In the case of the thick type I nanowires, TEM samples were prepared by transferring a water droplet containing nanowires from the substrate onto a carbon-coated copper grid. This procedure did not work very well for the thin nanowires. Furthermore, for the nanowires that grew in patterns on the substrate, it was necessary to identify where in the pattern a given section of nanowire had grown. It was therefore necessary to develop a new specimen preparation technique for plane-view studies of undisturbed surfaces using TEM (Foss *et al.*, 2010). This technique could be useful in general for studying grown nanowires or quantum dots, defects or patterns of objects/structures on a sample surface. Electrical measurements were performed using an atomic force microscope (AFM) with a conductive tip.

3. Results

3.1 Growth without a catalyst

Several attempts were made to induce self-organized growth without a catalyst (Hadzialic, 2004). In these we used plain or scratched Si and GaAs substrates as described above. Deposition rates varied from 2.5 - 45 Å/min. During HgTe deposition a few crystals grew

along scratches, but mostly there was no growth on the substrates. When a Cd flux was added, we obtained varying degrees of overgrown, polycrystalline HgCdTe layers, with more crystals along the scratches. No nanowires were found. Self-organized growth without a catalyst therefore does not seem to work.

3.2 Polycrystalline HgTe nanowires

VLS growth was then attempted using both Si, GaAs and CdZnTe substrates with Au particles. Fig. 1(a) shows a SEM image of HgTe nanowires (and platelets) grown on a Au-sputtered Si substrate. The uneven surfaces of the nanowires already hint at their polycrystalline nature, even though they look straight on a larger scale. The deposition rate was ~ 40 Å/min, the equivalent thin film thickness deposited 0.50 µm, and the growth temperature 178 °C. The wires are 100-500 nm wide and 1- 4 µm long, and they grow laterally on the surface with random orientation in the surface plane, which indicates that there is no epitaxial coupling to the substrate. This is supported by the fact that the wires are not firmly attached to the surface, as they were swept away by an AFM tip in contact mode. Furthermore, there is no visible Au droplet at the ends of the wires, as seen in TEM

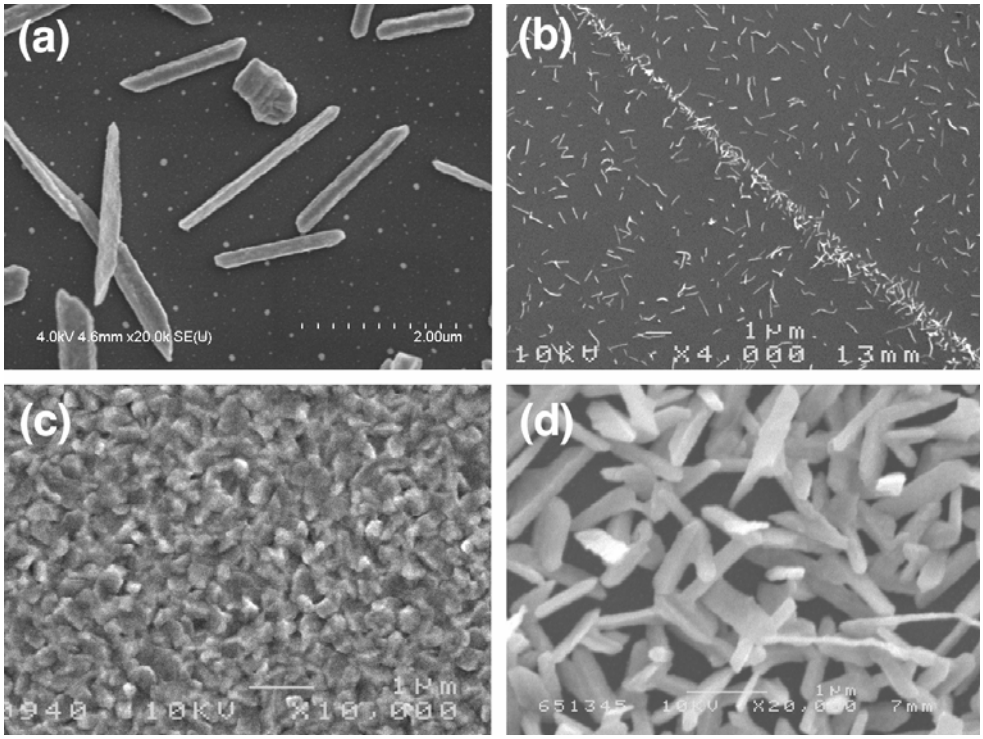

Fig. 1. SEM images of (a) and (b) different densities of HgTe nanowires grown on Au-sputtered Si substrates, (c) polycrystalline HgTe grown on a Au-sputtered Si substrate which was not etched before sputtering, (d) high density of HgTe nanowires grown on a Si substrate with a relatively thick sputtered Au layer.

or SEM images of nanowires grown by the VLS or VSS techniques in other materials. However, as described above, no wires formed on substrates without Au. We conclude that the wires have not grown by the VLS mechanism; instead we believe the Au particles function as nucleation centers for the nanowires. Possibly the Au particles can 'hold' Hg atoms until Te atoms arrive and nucleate a HgTe crystal. Once the crystal has nucleated, it grows by self-organization into a wire. These results are similar to the observations of Zhang *et al.* who used a Ti layer on a Si substrate for growth of IrO_2 nanowires (Zhang *et al.*, 2005). They did not observe Ti particles on the nanowires after growth and concluded the Ti just helped with nucleation.

The density of HgTe nanowires can vary a lot. A higher density of nanowires is observed along scratches in the substrate surface, as seen in Fig. 1(b). This is reasonable, as the surface energy necessary to nucleate a crystal in a scratch is lower. It is also possible that there is more Au in the scratch than outside. The scratches clearly help make nucleation sites. Most of the Au particles on the flat parts of the surface do not nucleate wires. This could be due to the size of the particle, or that the nucleation is very sensitive to the geometry of the particle.

On some substrates we did not remove the native oxide before Au sputtering; otherwise the normal growth process was performed on them. This resulted in a polycrystalline HgTe film, as seen in Fig. 1(c). Etched and Au sputtered substrates placed next to these substrates during growth had HgTe nanowires and no overgrown layer, similar to the wires on Figs. 1(a) and 1(b). Tests described below show that HgTe does not grow on SiO_2 at these growth conditions. We therefore believe that the oxide prevents diffusion of the Au, leaving Au nucleation sites all over the surface.

For etched and Au sputtered substrates we found a strong correlation between the density of wires and how many days the substrate had been kept in air after Au sputtering and before loading into the MBE machine. The sputtered Au layers are thin and porous, most likely allowing oxygen to react with the silicon surface. Also here the oxide probably impedes diffusion of Au during heating, resulting in more nucleation sites (or sites with a more favorable geometry) and a higher wire density. Other factors that affected the wire density were the Au layer thickness, where higher thickness gave higher density, as seen in Fig. 1(d), the trace of the RHEED beam on the surface (gave a different density of wires, but the density could be either lower or higher), and a rough ion milled surface before depositing the Au (gave a polycrystalline layer, probably due to impeding the Au diffusion). When the density is high, the wires also grow out from the substrate surface, as seen in Fig. 1(d).

A TEM image of some wires and their diffraction pattern are shown in Figs. 2(a) and 2(b), respectively. These wires were grown with a 10 °C higher substrate temperature than the wires in Fig. 1(a). The electron diffraction pattern shows that the nanowires are polycrystalline with lattice constants corresponding to HgTe with a sphalerite type crystal structure. The EDX spectrum from a small area of a different wire is shown in Fig. 2(c) (The Al peak comes from the sample holder). EDX analysis of nanowires on the Si substrates showed no Hg or Te between the wires. XPS analysis of a large substrate area containing wires gave a Hg:Te ratio of ~ 1:1.

Several variations in growth conditions were attempted in order to reduce polycrystallinity. Reduction of the deposition rate to ~ 1/3 resulted in no wires on the sample, which meant the incoming Te flux was too low compared to the Te re-evaporation rate. During three growth runs, attempts were made to nucleate the wires for 1 min or 5 min

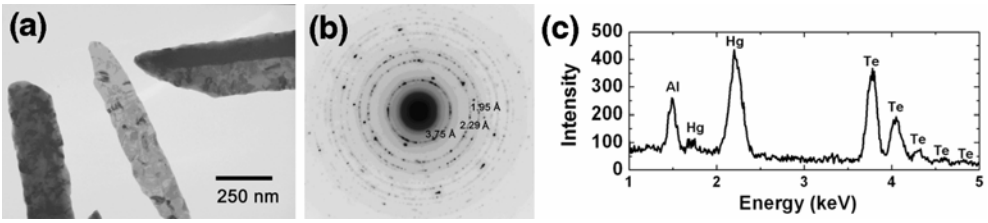

Fig. 2. (a) TEM image of HgTe nanowires, (b) electron diffraction pattern from the nanowires in (a), (c) EDX spectrum from a point on another HgTe nanowire that was transferred to a TEM carbon-coated Cu grid. (a) and (b) are taken from (Selvig *et al.*, 2006).

with normal Te flux, then turn down the flux to 50% or 70% for the rest of the growth. The idea was to inhibit nucleation of new grains by reducing the flux. This resulted in no (for 50 % flux) or fewer (70 % flux) wires that were still polycrystalline, and with random orientations on the substrate surface.

Raman scattering measurements were made at room temperature, as described in (Haakenaasen *et al.*, 2008a). In terms of lattice vibrations the alloy HgCdTe exhibits classic 'two-mode' behavior, which means that it behaves as though there were two sublattices present with their own phonon structures which evolve in frequency with x-value. The Raman spectrum from several wires clearly showed only the HgTe phonon modes. The scattering was strong, which indicates the crystal has well-defined electronic states. Furthermore, a relative sharpness of the longitudinal optical phonon indicates that the material has good crystallinity in the short range. As the wires are polycrystalline, this means that the crystallinity is good within the individual grains.

HgTe was also grown on Au-sputtered GaAs and CdZnTe substrates. Growth on GaAs substrates resulted in lateral HgTe nanowires and platelets similar to the ones on Si, but with a smaller average aspect ratio and slightly more rounded ends, as shown in Fig. 3(a). Growth on CdZnTe substrates resulted in a high density of nanocrystals with nanowires sticking out of the surface plane, as shown in Fig. 3(b). These nanowires grew out from the nanocrystals on the surface, and no epitaxial coupling to the substrate could be found.

The high density of crystals probably had something to do with substrate preparation, as occasional areas had a low density of lateral wires, similar to on Si or GaAs. Again, the explanation could be that Au did not diffuse as easily on the CdZnTe substrates.

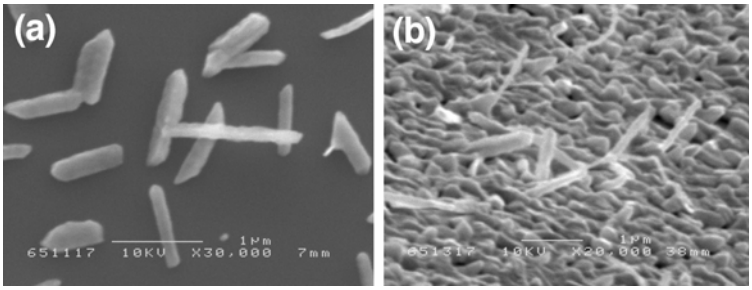

Fig. 3. (a) HgTe nanowires and platelets grown on a Au-sputtered GaAs substrate, (b) HgTe grains and nanowires grown on a Au-sputtered CdZnTe substrate.

3.3 Twisted, single crystal HgTe nanowires

Figs. 4(a) and 4(b) are SEM images of nanowires grown at 1/6 of the time of the wires in Fig. 1(a) (deposition rate 40 Å/min, equivalent film thickness 0.083 µm, growth temperature 186 °C). The wires or ribbons are 20-50 nm wide and 0.5-1 µm long, but not quite straight. These wires are thin enough that a positive band gap may have opened up, in which case they would be very interesting for IR devices. A bright field TEM image is shown in Fig. 4(c).

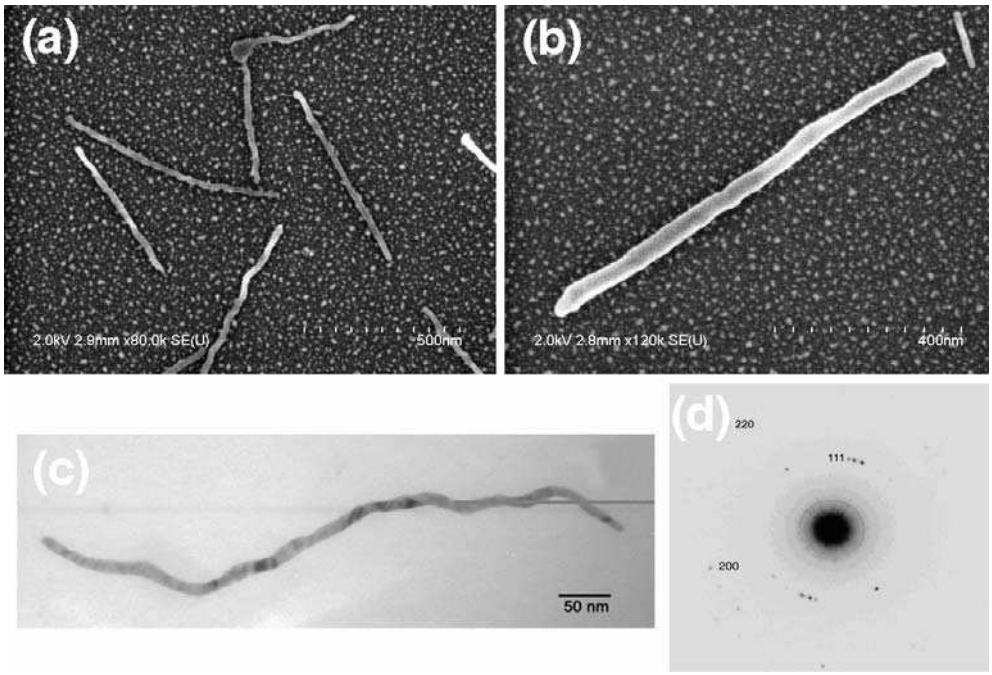

Fig. 4. (a) and (b): SEM images of thin, twisted nanowires grown on Au-sputtered Si substrates, c) Bright field TEM image of such a nanowire, d) electron diffraction pattern from the wire in c) plus another wire close by. The lattice constant (and extinction rules) is consistent with HgTe. a) is taken from (Haakenaasen *et al.*, 2008a), c) and d) are taken from (Selvig *et al.*, 2006).

A TEM diffraction pattern from the wire in Fig. 4(c) and a nearby wire is shown in Fig. 4(d). What at first looks like several grains in the wire, turns out on closer inspection to be bending contrast which moves when the wire is tilted with respect to the incoming electron beam. The wires seem to consist mainly of single crystal HgTe with the <111> direction oriented along the wire, but with bends in the wire (Haakenaasen *et al.*, 2008a).

Fig. 5 shows a TEM dark field image of a wire from a sample grown with 1/3 of the growth time used in Fig. 1(a); equivalent thin film thickness deposited was 0.17 µm. Lamellar twins by rotation around a <111> axis are clearly observed at a kink in the wire. This is commonly observed in MBE-grown HgCdTe (Selvig *et al.*, 1995).

The lateral nanowires can grow over each other, as seen in Figs. 1(a) and 3(a). This means that material can diffuse along the wire so that it grows in length. The height of both the

thin, twisted wires and the thicker polycrystalline wires is smaller than the total equivalent thin film thickness for the given growth, so clearly not all material deposited is incorporated into the wires. As a growth mechanism for the wires, we suggest that after nucleation at Au particles, only the atoms that land on the wires are incorporated. These atoms can diffuse both to the ends, making the wire longer, and fill in the 'corners' so that the wires get both wider and seemingly straighter with time. They add new grains instead of making old grains larger. In this way the wire side walls can become reasonably straight even though the wires are not single crystal.

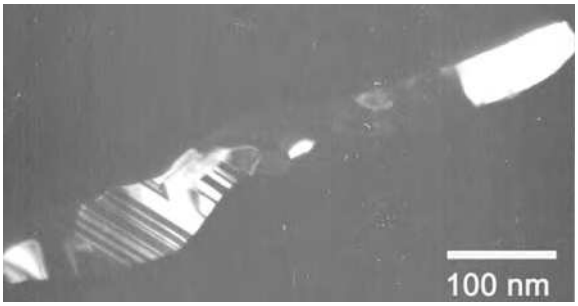

Fig. 5. TEM dark field image of a nanowire grown for approximately 1/3 of the time of the nanowires in Fig. 1(a). Twin defects can be observed. The 111 reflection was used to form the image. Taken from (Selvig *et al.*, 2006).

3.4 Segmented HgTe<111>/Te<001> nanowires

To test if the bending of the thin wires was due to interference between the growing nanowires and the Au particles, the Si substrates were patterned so that the Au particles were confined to certain areas, such as the array of 3.5-μm-diameter circles shown in Fig. 6(a). The SEM image shows nanowires that have nucleated and grown on and out from the Au particle areas. The growth conditions were the same as for the thin type II nanowires in Section 3.3. Fig. 6(b) is a higher magnification SEM image of a wire that grew from the inside to the outside of such an area. The wires are typically 15-70 nm wide and 0.5-1.5 μm long, and some of them may therefore have positive band gap. Wires that grew within the Au particle regions were uneven and not quite straight, while wires that grew out and away from the Au areas were straight and smooth, showing that the Au particles must indeed somehow block the straight growth of the wires. The straight wires were also often a little thicker at the end and had random orientation in the surface plane. These characteristics were common for the wires grown outward from various Au particle patterns. No wires grew entirely outside the Au particle areas, as the Au particles are necessary to nucleate the growth.

In order to find out if the sections of wire growing inside and outside a Au particle region were different, it was necessary to retain the surface pattern of Au particles and wires. Samples were prepared according to the inclined pseudo-plane-view specimen preparation technique developed for this purpose, as described in (Foss *et al.*, 2010). The TEM image of a wire growing on the border of a Au particle area is shown in Fig. 7(a) and a selected area

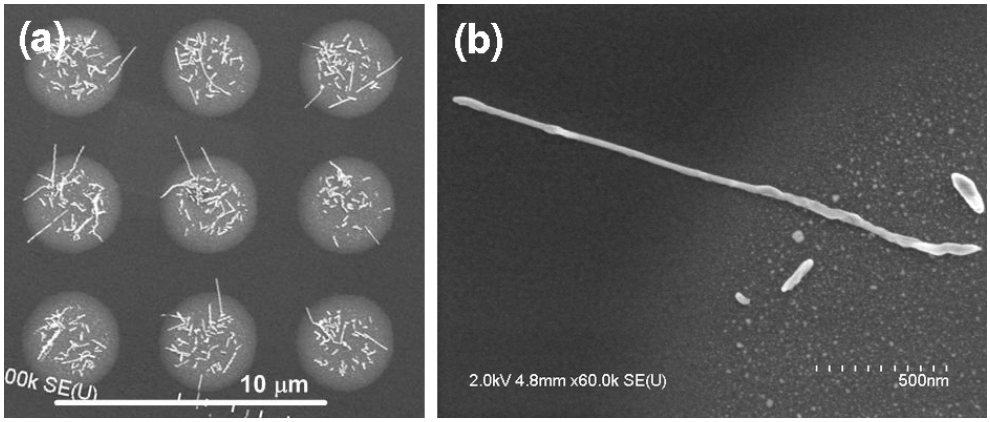

Fig. 6. SEM images of (a) HgTe nanowires that have grown on circular areas with Au particles on a Si substrate, and (b) a nanowire that has grown from the inside to the outside of such a Au particle area. (b) is taken from (Haakenaasen *et al.*, 2008b).

diffraction (SAD) pattern from the wire in Fig. 7(b). Although there are some Au particles where the wire has grown, they are very small and the wire is quite straight and relatively smooth. We see from the SAD pattern, which is from the right half of the middle of the wire (including a little of the dark region at the tip), that the hexagonal Te <001> direction is parallel to the cubic HgTe <111> direction and parallel to the wire axis. This was confirmed in all our TEM observations. EDX spectra were taken from 100 nm large areas along the wire. The spectrum from the dark tip is shown in Fig. 7(c). It contains peaks from Hg and Te (in addition to Si from the substrate and Cu from the grid) and is consistent with HgTe. A spectrum from the middle of the wire is shown in Fig. 7(d). It shows only Te peaks and thus is consistent with elemental Te. (The small peaks at 2.1 and 9.7 keV are due to Au from the Au particles). We notice that the tip of the wire is darkest, consistent with HgTe since Hg is a stronger scatterer than Te. The opposite end of the wire gives a similar spectrum to the one in Fig. 7(c), providing evidence for HgTe also there. This end seen in the image is not necessarily the true tip of the wire as the tip may have been ion milled away during TEM preparation (it is right next to the ion milled hole in the Si substrate). Fig. 7(e) shows another wire that has grown out of a Au particle area. The left one third of the wire is inside the Au particle area, the rest outside. EDX spectra show that also this wire has HgTe at the two ends. Between the ends the spectra indicate alternating sections of Te and HgTe.

The wires thus consist of HgTe at the ends and mostly Te segments (but some HgTe segments) in the middle. The segmentation is consistent with the Hg-Te phase diagram if the average composition is too low in Hg. According to this phase diagram, HgTe is a line compound with no other phases between elemental Te and HgTe. It is interesting that the bulk phase diagram seems to apply also for nanowires. Since the wires grow mainly at the ends, material that lands on the wires must diffuse to the ends before being incorporated into the crystal lattice. During MBE growth of Hg(Cd)Te there is a very large flux of Hg, as the Hg atoms have a very low sticking coefficient. It is likely that Hg atoms re-evaporate

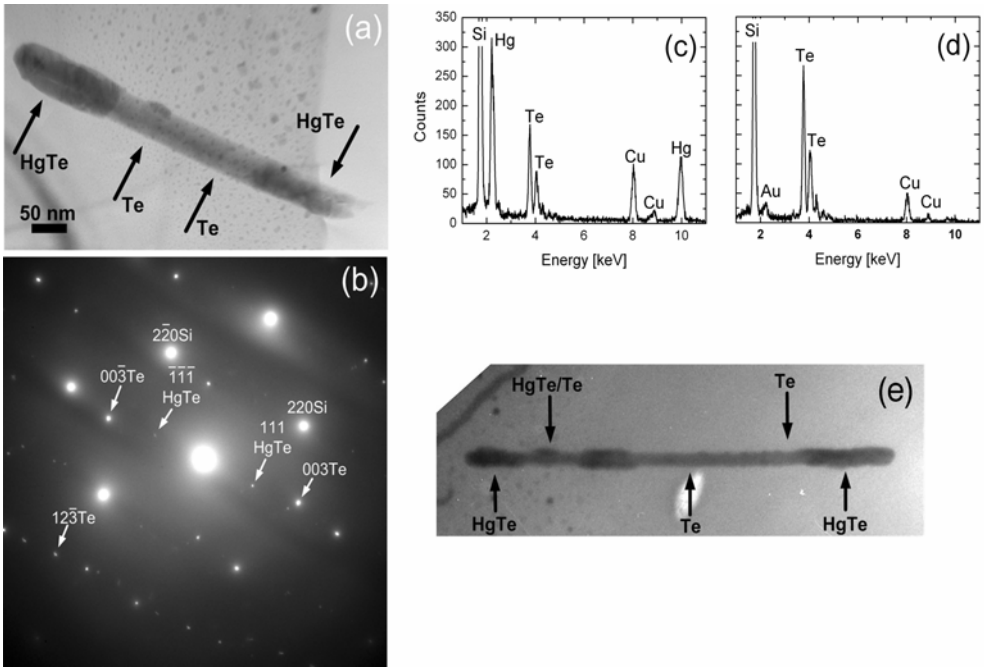

Fig. 7. (a) Bright field TEM image of a nanowire that has grown on the border of a Au particle area, (b) SAD pattern from the right half of the middle of the wire (including some of the darker region at the tip), (c) EDX spectrum from the dark tip on the left side of the wire, (d) EDX spectrum from the middle region of the wire, and (e) Bright field TEM image of a different, 1 μm long nanowire that has grown from the inside to the outside of a Au particle area. All figures taken from (Haakenaasen *et al.*, 2008b).

quickly rather than diffuse, whereas Te atoms are known to diffuse far on a Hg(Cd)Te film surface during growth. We therefore believe that the Te atoms diffuse along the wires to the ends, where there is Hg available to grow HgTe. The lack of Hg in parts of the wire could be due to less Hg being incorporated during growth of nanowires than thin films or that Hg evaporates from already grown sections of the wire during further growth of the wire.
The lattice constant of the cubic HgTe is 6.46 Å, while for hexagonal Te the lattice constants are a = 4.46 Å and c = 5.93 Å. Although HgTe and Te have completely different crystal structures (this is not like the stacking fault alternation of the cubic zincblende and hexagonal wurtzite crystal structures that is seen in many compound semiconductor nanowires grown by the VLS mechanism), both the (111) plane of HgTe and the (001) plane of Te have a six-fold symmetry. The d_{220} spacing of HgTe is 2.28 Å while the d_{110} spacing of Te is 2.23 Å, resulting in a lattice mismatch of ~ 2%. Although this would be a large. mismatch for thin films, heterostructured nanowires can accommodate larger mismatch and still be free from dislocations or other defects because the small lateral dimension allows

efficient strain relaxation (Thelander *et al.,* 2004). The segments of HgTe and Te therefore can accommodate good epitaxial match.

3.5 Au and Te nanowires

On a few of the samples there were small areas with a different type of nanowire. While the HgTe wires looked black in the optical microscope, these wires looked white. SEM micrographs and EDX analysis revealed that these wires were very straight and smooth and consisted of Te, Figs. 8(a) and 8(b). They could appear both in a 'bird's nest' or as individual lateral nanowires on the substrate. It is not clear what caused these Te nanowires to grow instead of the HgTe nanowires.

For a thicker Au sputter layer (60 Å), the growth resulted in long (10-40 µm) Au wires along the <110> directions, in addition to the HgTe wires, Fig. 8(c). The Au wires are the result of Au diffusing to steps on the Si(100) surface, as shown by fewer Au particles in the immediate vicinity of these wires. There was generally no growth of HgTe nanowires from the long Au wires. It is possible that the geometry was not conducive to nucleation or that the volume of these wires is so large that the concentration of dissolved Hg was too low for nucleation.

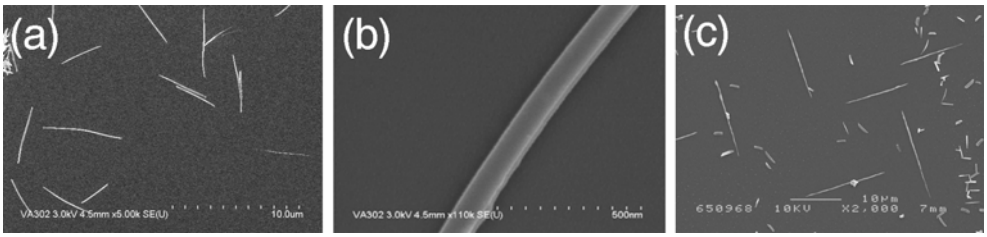

Fig. 8. SEM images of (a) and (b)Te nanowires grown on a Au-sputtered Si substrate, and (c) long Au wires in addition to HgTe nanowires grown on a Au-sputtered Si substrate. (b) is taken from (Haakenaasen *et al.*, 2008a).

3.6 Attempts to grow HgCdTe nanowires

Several attempts to grow $Hg_{0.75}$ $Cd_{0.25}Te$ nanowires on Au-coated Si substrates were made with varying Au thickness, deposition rate (22 – 44 Å/min) and total deposited thickness (1760 – 5280Å). All growths resulted in a polycrystalline HgCdTe layer and no nanowires. A low deposition rate (10 Å/min) of CdTe at 340°C only resulted in Au particles and no growth of CdTe.

3.7 Explanation why VLS does not work

To try to understand why HgTe or HgCdTe nanowires did not grow by the VLS or VSS techniques, a comparison to the growth of Au-catalyzed GaAs nanowires was made (Tibballs, 2005). Persson *et al.* grow their GaAs wires at 540°C, but they have found that the Au catalyst particle is solid during growth (Persson *et al.* 2004). The VSS technique still works as enough Ga and As can diffuse through and around the Au particle. There is no phase diagram available for HgTe-Au or HgCdTe-Au, but we can get some information

from the Cd-Au and Hg-Au phase diagrams (Morfatt, 1977). In Au-Hg, the melting point depression gives a solidus temperature of 419°C at 20 at.% Hg. At ~200°C, which is the Hg(Cd)Te MBE growth temperature, a 97 at.% Hg concentration in Au is needed for the Hg-Au solution to be fully liquid. However, at 200°C Au can dissolve at most 15 at.% Cd and Hg, and supersaturation will cover the Au particle with intermetallic phases, effectively capping the particle. This will probably prevent more Hg or Cd dissolving in the Au, so that the particle does not reach the high Hg concentration needed for this solution to become liquid. The VLS mechanism can therefore be excluded. Furthermore, intermetallic phases usually reduce diffusion, so the capping layer may prevent or at least impede further transport of Hg or Cd through the Au.

There is no published data on diffusion coefficients of Cd or Hg in Au, but employing the activation energies for Zn and Sn in (Mortlock & Rowe, 1965) as a guide, because these elements exhibit similar atomic size and solubility in Au, we note that one expects a six-order-of-magnitude reduction in diffusivity when going from 540°C to 200°C. We therefore believe the diffusion of Hg and Cd through Au is too slow even with the highest concentration gradient consistent with not precipitating intermetallics on the surface. We would need a growth temperature of approximately 420°C to attain a diffusivity comparable with the GaAs experiment, but this temperature is not compatible with the Hg fluxes available in the MBE chamber. Several other groups have reported growth of other II-VI VLS nanowires (without Hg) at around 400°C (Shan *et al.*, 2005; Janik *et al.*, 2006). An additional problem is that Au and Te form a solid phase at 200°C, which will compete with growth of HgTe. An additional problem for HgCdTe is that there is a large difference in stability between HgTe and CdTe, which means it will be very difficult to control the ratio between Hg and Cd in the grown crystal. There would have to be a very low Cd concentration in Au in equilibrium with HgCdTe; otherwise all Te would be bound to Cd and the crystal would become almost entirely CdTe. But such a low concentration would exclude enough transport of Cd through the Au particle. Looking for other possible catalyst materials, we find that Ag is not much better than Au, while In or Pb probably will precipitate a phase with Te. The only possibility at 200°C seems to be thallium, which we do not want in our growth chamber. Excluding thallium, we conclude that it is not possible to make HgTe or HgCdTe nanowires via VLS or VSS at the MBE growth temperature.

3.8 Selective growth using a SiO_2 mask

To investigate the possibility of selective growth, HgCdTe and HgTe were grown on a series of Si and CdZnTe substrates with and without a SiO_2 mask (Hadzialic, 2004). The HgCdTe and HgTe deposition rates were varied by a factor 100, from 1.3 to 135 Å/min, and EDX and XPS were used to determine if any growth had occurred. HgCdTe grew on SiO_2 for all except the lowest deposition rates (incompatible with realistic growth rates) while HgTe did not grow on SiO_2 for any deposition rate. SiO_2 can therefore be used as a mask for selective growth of HgTe, but not for HgCdTe.

3.9 Electrical characterization using conductive atomic force microscopy

To perform electrical measurements on a single nanowire, it is necessary to have two or more contacts to the wire. This is no trivial task since the wires are so small. Electron beam

lithography (EBL) has been used on wires made in other materials, but HgTe will degrade or evaporate at the normal temperatures used for baking of EBL resists. An alternative method has been developed to obtain the circuit illustrated in Fig. 9(a). Large, sputtered Au electrodes were deposited, using optical lithography, on a sample with randomly distributed, polycrystalline type I HgTe nanowires, shown in Fig. 9(b). Some wires were partly covered by the Au electrode. A conductive AFM tip could then be used as a second, movable electrode to measure current-voltage (I-V) curves at several positions L along such

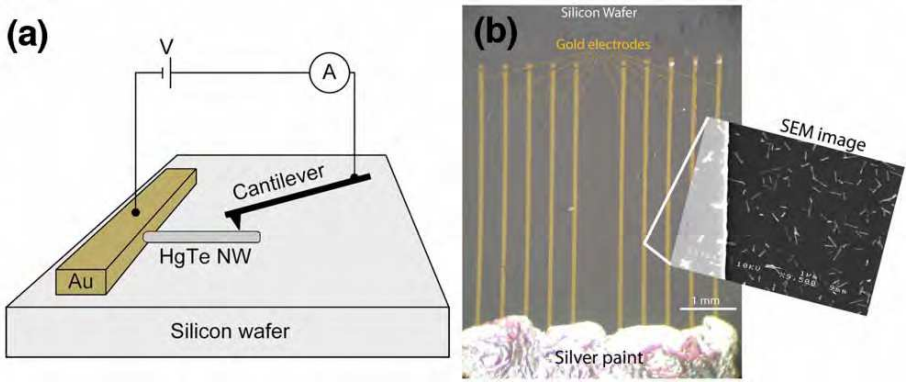

Fig. 9. (a) Schematic drawing of the nanowire-conductive AFM electrical circuit. (b) Optical microscope image of sputtered gold electrodes on a Si substrate with HgTe nanowires. Inset is an enlarged SEM image which shows randomly distributed HgTe nanowires, some of which are partly covered by the gold electrode.

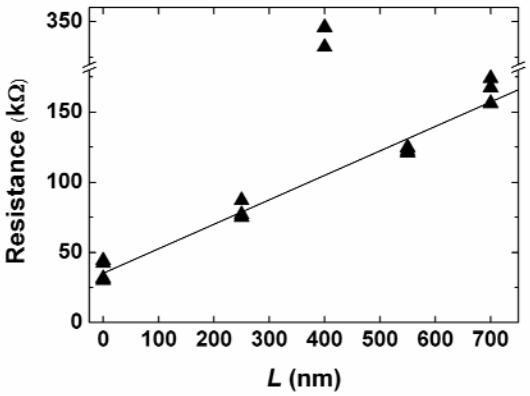

Fig. 10. The resistance values from the measured I-V curves for one nanowire, and a linear fit to the data (excluding the data points at L = 400 nm). Taken from (Gundersen et al., 2010).

wires. The I-V curves were linear and the resistance was found from the slope of linear fits to the data. Then all these measured resistance values were plotted vs. L, as shown in Fig. 10. Also these data were very well fitted with straight lines (excluding the points at L = 400 nm, where the tip had poor contact to the wire), and the slope dRmeasured/dL was extracted for each wire.

In the measurement circuit it was only the drift resistance of the wire that varied with L; therefore the wires were found to be diffusive (in the ballistic regime the resistance is independent of wire length). From the slopes dRmeasured/dL and the cross-section of the wires, resistivities were calculated for two wires. These were ~ 250/130 times larger than the resistivity 4.4×10^{-4} Ωcm of an MBE-grown 3 μm thick HgTe film, as measured by the van der Pauw technique. The difference is attributed to scattering at the grain boundaries and the surface. These measurements are described in more detail in (Gundersen, 2008; Gundersen et al., 2010).

4. Further work

To obtain straight, single crystal HgTe nanowires, the growth conditions should be varied to obtain a higher Hg content in the wires growing away from the Au particle areas. Electrical and optical characterization of the different types of wires is the next step. Resistivity measurements should be made on the type II and type III HgTe/Te wires described above. A Schottky curve could be an indication of a band gap or barrier in the wire. Measurements should be performed at small *L* to try to observe ballistic transport. The substrate could be used as a common back-gate electrode to modulate the carrier density of the wires, thereby providing information about the doping type of the wire. If two contacts could be made by EBL, the sample could be mounted in a cryostat. If the effective width of a wire in the ballistic regime could be controlled by a gate voltage, then conductance quantization could perhaps be observed at lower temperatures. Photoluminescence or photoconductive measurements could determine the effective band gap of Te nanowire segments and reveal whether a positive band gap has opened up in thin HgTe wires. This would open up for electro-optic devices in the infrared region of the spectrum. To stabilize the wires, a thin CdTe passivation layer could be grown *in-situ*. Spintronics and thermoelectric applications could also be considered.

5. Conclusions

HgTe nanowires nucleated by Au particles have been grown on Si and GaAs substrates by molecular beam epitaxy. The wires grow laterally on the surface, but they are not epitaxially coupled to the substrate. During the initial growth, Au particles on the surface block the straight, forward growth of the wires, resulting in twisted, but mostly single crystal, <111>-oriented wires. During further growth, atoms can diffuse along the wires, both making them longer and filling in corners to make them wider and straighter. New grains are added so that the larger wires end up polycrystalline. Raman scattering experiments show that the crystallinity is good within the individual grains. When the growing wires are unimpeded by Au particles, they become straight and smooth, and they consist of segments of cubic <111>HgTe and hexagonal <001>Te parallel to the wire axis.

Attempts at including Cd to grow HgCdTe on Au-coated substrates resulted in a polycrystalline layer and no nanowires. By comparing to Au-catalyzed growth of GaAs nanowires, we conclude that the diffusion coefficients of Cd and Hg through Au are too low for the VLS mechanism to function at the low HgCdTe MBE growth temperature. SiO_2 can be used as a mask for selective growth of HgTe, but not for HgCdTe. A new sample preparation technique for plane-view studies of undisturbed surfaces using TEM has been developed. The conductive tip of an AFM was used as a movable electrode to measure the resistivity of the thick, polycrystalline HgTe nanowires. Two nanowires were found to have diffusive electron transport, with resistivities two orders of magnitude larger than that of a HgTe film. The difference can be explained by scattering at the rough surface walls and at the grain boundaries in the wires.

6. Acknowledgements

The work was funded by Norwegian Ministry of Defence. Support for nanowire characterization was provided by the AFOSR under grant number FA9550-06-1-0484, P00002.

7. References

Björk, M. T.; Ohlsson, B. J.; Sass, T.; Persson, A. I.; Thelander, C.; Magnusson, M. H.;Deppert, K.; Wallenberg, L. R. & Samuelson, L. (2002). One-dimensional heterostructures in semiconductor nanowhiskers. *Appl. Phys. Lett.* 80, 6, (Feb. 2002), 1058-1060, 0003-6951.

Carter, R.; Sloan, J.; Kirkland, A. I.; Meyer, R. R.; Lindan, P. J. D.; Lin, G.; Green, M. L. H.;Vlandas, A.; Hutchinson, J. L. & Harding, J. (2006). Correlation of structural and electronic properties in a new low-dimensional form of mercury telluride. *Phys. Rev. Lett.* 96, 21, (Jun. 2006), 215501, 0031-9007.

Colin T. & Skauli, T. (1997). Applications of thermodynamical modelling in molecular beam epitaxy of $Cd_xHg_{1-x}Te$. *J. Electron. Mater.* 26, 6, (Jun. 1997), 688-696, 0361-5235.

Dheeraj, D. L.; Patriarche, G.; Largeau, L.; Zhou, H. L.; van Helvoort A. T. J.; Glas, F.; Harmand, J. C.; Fimland B. O. & Weman H. (2008). Zinc blende GaAsSb nanowires grown by molecular beam epitaxy. *Nanotechnology* 19, 27, (Jul. 2008), 275605, 0957-4484.

Dresselhaus, M. S.; Lin, Y.-M.; Rabin, O. & Dresselhaus, G. (2003). Bismuth nanowires for thermoelectric applications. *REPORTS: Nanoscale and Microscale Thermophysical Engineering*, 7, 3, (Jul. 2003), 207-219, 1089-3954.

Duan, X. & Lieber, C. M. (2000). The general synthesis of compound semiconductor nanowires. *Adv. Mater.* 12, 4, (Feb. 2000), 298-302, 0935-9648.

Foss, S.; Taftø, J. & Haakenaasen, R. (2009). A specimen preparation technique for plane-view studies of surfaces using transmission electron microscopy. *J. Electron Microscopy*, 59, 1, (Feb. 2010), 27-31, 0022-0744.

Green, M; Wakefield, G. & Dobson, P. J. (2003). A simple metalorganic route to organicallypassivated mercury telluride nanocrystals. *J. Mater. Chem.* 13, 5, (May 2003), 1076-1078, 0959-9428.

Gudiksen, M. S.; Lauhon, L. J.; Wang, J.; Smith, D. C. & Lieber, C. M. (2002). Growth of nanowire superlattice structures for nanoscale photonics and electronics. *Nature* 415, 6872, (Feb. 2002), 617-620, 0028-0836.

Gundersen, P. (2008). *Electrical characterization of HgTe nanowires using conductive atomic force microscopy*, Master's thesis, Dept. of Physics, Norwegian University of Science and Technology, Trondheim.

Gundersen, P.; Kongshaug, K. O.; Selvig E. & Haakenaasen, R. (2010). Electrical characterization of HgTe nanowires using conductive atomic force microscopy. In preparation.

Hadzialic, S. (2004). *Growth and Characterization of $Cd_xHg_{1-x}Te$ Nanowires*, Cand. Scient. thesis, Dept of Physics, University of Oslo, Oslo.

Haakenaasen, R.; Selvig, E.; Hadzialic, S.; Skauli, T.; Hansen, V.; Tibballs, J. E.; Trosdahl-Iversen, L.; Steen, H.; Foss, S.; Taftø, J.; Halsall, M. & Orr, J. (2008a). Nanowires in the CdHgTe material system. *J. Elec. Mater.* 37, 9, (Sep. 2008), 1311-1317, 0361-5235.

Haakenaasen, R.; Selvig, E.; Foss, S.; Trosdahl-Iversen, L. & Taftø, J. (2008b). Segmented nanowires of HgTe and Te grown by molecular beam epitaxy. *Appl. Phys. Lett.* 92, 13, (Mar. 2008), 133108-1 - 133108-3, 0003-6951.

Janik, E.; Sadowski, J.; Dluzewski, P.; Kret, S.; Baczewski, L. T.; Petroutchik, A.; Lusakowska, E.; Wrobel, J.; Zaleszczyk, W.; Karczewski, G.; Wojtowicz, T. & Presz, A. (2006). ZnTe nanowires grown on GaAs(100) substrates by molecular beam epitaxy. *Appl. Phys. Lett.* 89, 13, (Sep. 2006), 133114, 0003-6951.

Konig, M.; Wiedmann, S.; Brune, C.; Roth, A.; Buhmann, H.; Molenkamp, L. W.; Qi, X. L.; and Zhang, S. C. (2007). Quantum spin hall insulator state in HgTe quantum wells. *Science* 318, 5851, (Nov. 2007), 766-770, 0036-8075.

Morfatt, W. G. (1977). *The handbook of binary phase diagrams,* General Electric Company, 0-931690-00-5, Schenectady.

Mortlock, I. & Rowe, A. H. (1965). Atomic diffusion of mercury in gold. *Philos. Mag.* 11, 114 (1965) 1157-1164, 1478-6435.

Ohlsson, B. J.; Björk, M. T.; Magnusson, M. H.; Deppert, K.; Samuelson, L. & Wallenberg, L. R. (2001). Size-, shape-, and position-controlled GaAs nano-whiskers. *Appl. Phys. Lett.* 79, 20, (Nov. 2001), 3335-3337, 0003-6951.

Persson, A. I.; Larsson, M. W.; Stenstrom, S.; Ohlsson, B. J.; Samuelson, L. & Wallenberg, L. R. (2004). Solid-phase diffusion mechanism for GaAs nanowire growth. *Nature Mater.* 3, 10, (Oct. 2004), 677-681, 1476-1122.

Qin, A.-M.; Fang, Y.-P. & Su, C.-Y. (2007). Hydrothermal synthesis of HgTe rod-shaped nanocrystals. *Mater. Lett.* 61, 1, (Jan. 2007), 126-129, 0167-577X.

Ranga Roa A. & Dutta, V. (2006). Nanotubes in spray deposited nanocrystalline HgTe:I thin films. *Mater. Res. Symp. Proc.* 901E, 0901-Ra11-19 - Rb11-19.1- 0901-Ra11-19 - Rb11-19.6, 0272-9172.

Selvig, E.; Gjønnes, K.; Olsen, A.; Colin, T. & Løvold, S. (1995). TEM study of (Cd,Hg)Te grown by molecular beam epitaxy. *Inst. Phys. Conf. Ser.* 146, pp. 317-320, 0951-3248, Oxford 1995, IOP Publishing Ltd., Bristol.

Selvig, E.; Hadzialic, S.; Haakenaasen, R.; Skauli, T.; Steen, H.; Hansen, V.; Trosdahl-Iversen, L.; van Rheenen, A. D. & Lorentzen, T. (2006). Growth of HgTe nanowires. *Phys. Scripta* T126, (2006), 115-120, 0031-8949.

Selvig, E.; Tonheim, C. R.; Kongshaug, K. O.; Skauli, T.; Lorentzen, T. & Haakenaasen, R. (2007). Defects in HgTe grown by molecular beam epitaxy on (211)B-oriented CdZnTe substrates. *J. Vac. Sci. Technol. B* 25, 6, (Nov./Dec. 2007), 1776 -1784, 1071-1023.

Selvig, E.; Tonheim, C. R.; Kongshaug, K. O.; Skauli, T.; Hemmen, H.; Lorentzen, T. & Haakenaasen, R . (2008a). Defects in CdHgTe grown by molecular beam epitaxy on (211)B-oriented CdZnTe substrates. *J. Vac. Sci. Technol. B* 26, 2, (Mar./Apr. 2008), 525-533, 1071-1023.

Selvig, E.; Tonheim, C.R.; Lorentzen, T.; Kongshaug, K. O.; Skauli, T. & Haakenaasen, R. (2008b). Defects in HgTe and CdHgTe grown by molecular beam epitaxy. *J. Elec. Mater.* 37, 9, (Sep. 2008), 1444 – 1452, 0361-5235.

Shan, C. X.; Liu, Z. & Hark, S. K. (2005). Highly oriented zinc blende CdSe nanoneedles. *Appl. Phys. Lett.* 87, 16, (Oct. 2005), 163108, 0003-6951.

Song, H.; Cho, K.; Kim, H.; Lee, J. S.; Min, B.; Kim, H. S.; Kim, S.-W.; Noh, T. & Kim, S. (2004). Synthesis and characterization of nanocrystalline mercury telluride by sonochemical method. *J. Cryst. Growth* 269, 2-4, (Sep. 2004), 317-323, 0022-0248.

Tang, B.; Yang, F.; Ciu, Y.; Zhuo, L.; Ge, J. & Cao, L. (2007). Synthesis and characterization of wavelength-tuneable, water-soluble, and near-infrared-emitting CdHgTe nanorods. *Chem. Mater.* 19, 6, (Feb. 2007), 1212-1214, 0897-4756.

Thelander, C.; Björk, M. T.; Larsson M. W.; Hansen A. E.; Wallenberg, L. R. & Samuelson L. (2004). Electron transport in InAs nanowires and heterostructure nanowire devices. *Solid State Commun.* 13, 9-10, (Sep. 2004), 573-579, 0038-1098.

Tibballs, J. E. (2005). Scandinavian Institute of Dental Materials, Haslum. Private communication.

Tonheim, C. R.; Selvig, E; Nicolas, S.; Gunnæs, A. E.; Breivik, M. & Haakenaasen, R. (2008). Excitation density dependence of the photoluminescence from $Cd_xHg_{1-x}Te$ multiple quantum wells. *J. Phys: Conf. Series.* 100, 042024, 1742-6588, Stockholm June 2007, IOP Publishing Ltd., Bristol.

Wagner, R. S. & Ellis, W. C. (1964). Vapor-liquid-solid mechanism of single crystal growth. *Appl. Phys. Lett.* 4, 5, (Mar. 1964), 89-90, 0003-6951.

Wu, Y.; Fan, R. & Yang, P. (2002). Block-by-block growth of single-crystalline Si/SiGe superlattice nanowires. *Nano. Lett.* 2, 2, (Feb. 2002), 83-86, 1530-6984.

Yang, J; Zhou, Y.; Zheng, S.; Liu, X.; Qiu, X.; Tang, Z.; Song, R.; He, Y.; Ahn, C. W. & Kim J. W. (2009). Self-reorganization of CdTe nanoparticles into near-infrared $Hg_{1-x}Cd_xTe$ nanowire networks. *Chem. Mater.* 21, 14, (Jul. 2009), 3177-3182, 0897-4756.

Zhang, F.; Barrowcliff, R.; Stecker, G.; Wang, D. & Hsu, S.-T. (2005). IrO_2 nano structures by metal organic chemical vapor deposition, *NSTI-Nanotech 2005 Conf. Proc. 2,* pp. 623-626, 0-9767985-4-9, Anaheim, May 2005, Nano Science and Technology Institute, Cambridge.

Nanowires

Edited by Paola Prete

ISBN 978-953-7619-79-4
Hard cover, 414 pages
Publisher InTech
Published online 01, February, 2010
Published in print edition February, 2010

This volume is intended to orient the reader in the fast developing field of semiconductor nanowires, by providing a series of self-contained monographs focusing on various nanowire-related topics. Each monograph serves as a short review of previous results in the literature and description of methods used in the field, as well as a summary of the authors recent achievements on the subject. Each report provides a brief sketch of the historical background behind, the physical and/or chemical principles underlying a specific nanowire fabrication/characterization technique, or the experimental/theoretical methods used to study a given nanowire property or device. Despite the diverse topics covered, the volume does appear as a unit. The writing is generally clear and precise, and the numerous illustrations provide an easier understanding of the phenomena described. The volume contains 20 Chapters covering altogether many (although not all) semiconductors of technological interest, starting with the IV-IV group compounds (SiC and SiGe), carrying on with the binary and ternary compounds of the III-V (GaAs, AlGaAs, GaSb, InAs, GaP, InP, and GaN) and II-VI (HgTe, HgCdTe) families, the metal oxides (CuO, ZnO, ZnCoO, tungsten oxide, and PbTiO3), and finishing with Bi (a semimetal).

InTech Europe
University Campus STeP Ri
Slavka Krautzeka 83/A
51000 Rijeka, Croatia
Phone: +385 (51) 770 447
Fax: +385 (51) 686 166
www.intechopen.com

InTech China
Unit 405, Office Block, Hotel Equatorial Shanghai
No.65, Yan An Road (West), Shanghai, 200040, China
中国上海市延安西路65号上海国际贵都大饭店办公楼405单元
Phone: +86-21-62489820
Fax: +86-21-62489821